



Addition of catalysts to magnesium hydride by means of cold rolling

S.D. Vincent, J. Lang, J. Huot*

Institut de Recherche sur l'Hydrogène, Université du Québec à Trois-Rivières, 3351 Boul. des Forges, Trois-Rivières, Québec, Canada, G9A 5H7

ARTICLE INFO

Article history:

Received 27 July 2011

Received in revised form

20 September 2011

Accepted 22 September 2011

Available online 4 October 2011

Keywords:

Magnesium hydride

Cold rolling

Catalyst

Crystallite size

Strain

ABSTRACT

In this paper we compare the techniques of cold rolling and ball milling as a mean to synthesized nanocomposites $MgH_2 + 2 \text{ at.}\%X$ where $X = \text{Co, Cr, Cu, Fe, Mn, Nb, Ni, Ti, V}$. High energy ball milling was performed under argon for 30 min while cold rolling was done in air with a number of roll limited to five. Particle and crystallite sizes are smaller in the ball milled compounds than in the cold rolled ones. The hydrogen sorption kinetics of the ball milled compounds was also faster than the cold rolled samples but not by a wide margin. Because cold rolling was done in air, this limited the number of rolls that could be performed. It is expected that rolling under protective atmosphere will enable a higher number of rolls and better sorption kinetics.

© 2011 Elsevier B.V. All rights reserved.

1. Introduction

Despite its high temperature of operation and slow kinetics, magnesium is still considered as a candidate for some hydrogen storage applications. Over the years, it has been well established that ball milling greatly enhances the hydrogen sorption kinetics of Mg and Mg-based alloys and is a good way to form nanocomposites with elemental catalysts [1–8]. However, using high energy milling for industrial level production could be expensive in terms of capital and operation costs. Consequently, there is a need to investigate other means of synthesis/modification of metal hydrides that could be easily scaled-up to industrial level. In this respect, severe plastic deformation (SPD) techniques should be examined.

In the past few years, SPD techniques such as equal angular channel pressing (ECAP), high pressure torsion (HPT), forging, and cold rolling have been investigated as means to synthesize and process metal hydrides, especially magnesium-based compounds [9–20] and Ti-based alloys [21–24].

Recently, it has been shown by Leiva et al. [25] and by Lang and Huot [26] that SPD could also be performed on the fully hydrided material and that the end product shows a nanocrystalline structure similar to the one obtained by ball milling. In the Lang and Huot investigation the rolling and all other handling were performed in air without important reduction of capacity or kinetic. More details on the effect of air exposure are reported in Ref. [27]. In this paper

we report the use of cold rolling to add transition metals catalysts to magnesium hydride. As a means of comparison, a parallel study was made by using ball milling to synthesize the same compounds. The effects on the morphology, crystal structure and hydrogen storage properties of addition of catalysts by cold rolling in air and ball milling in argon were investigated.

2. Experimental method

The cold-rolling apparatus used in this study was a Durston DRM 130 modified in such a way that vertical milling is possible. This configuration enables the processing of powder samples. As starting material we used 300 mesh (50 μm) MgH_2 powder (98% purity) from Alfa Aesar. This MgH_2 powder was hand mixed with 2 at.% of transition metal powder. Elements studied were: Co, Cr, Cu, Fe, Mn, Nb, Ni, Ti, V. Details on purities and powder size are in Table 1. Cold rolling was performed by inserting the powder mixtures between two 316 stainless steel plates to prevent contamination from the rolls. All rollings were performed in air. After each rolling pass, the powder was collected and rolled again to the final numbers of rolls. Milling was carried out on a Spex 8000 high energy mill in a hardened steel crucible with a powder to ball ratio of 1/10. For milled samples, all handlings, loading and closing of crucible were made in an argon atmosphere glove box.

The hydrogen sorption properties were measured with a Sieverts-type apparatus. All measurements were performed at 623 K with a hydrogen pressure of 2000 kPa for absorption and 35 kPa for desorption. Crystal structure was analyzed from X-ray powder diffraction patterns registered on a Bruker D8 Focus apparatus with $\text{CuK}\alpha$ radiation. Phase abundances as well as crystallite

* Corresponding author. Tel.: +1 819 376 5011x3576; fax: +1 819 376 5164.
E-mail address: jacques.huot@uqtr.ca (J. Huot).

Table 1
Manufacturer, purity, and powder size of catalysts studied.

| | Co | Cr | Cu | Fe | Mn | Nb | Ni | Ti | V |
|-------------------------------|------------|---------|------------|------------|---------|------------|---------|------------|---------|
| Manufacturer | Alfa Aesar | Aldrich | Alfa Aesar | Alfa Aesar | Aldrich | Alfa Aesar | Aldrich | Alfa Aesar | Aldrich |
| Purity (%) | 99.5 | 99 | 99 | 98 | 99.9 | 99.8 | 99.99 | 99.5 | 99.5 |
| Powder size (μm) | 44 | 44 | 44 | 44 | 297 | 1–5 | 149 | 44 | 44 |

size and microstrain were evaluated from Rietveld method using Topas software [28] via the fundamental parameter approach [29].

3. Results

3.1. Crystal structure

The crystal structure of all synthesized samples was determined from Rietveld refinement of their X-ray powder diffraction patterns. As all samples produced from a given technique share common features only one representative composition is discussed. In Fig. 1 the X-ray powder diffraction patterns of $\text{MgH}_2 + 2 \text{ at.}\% \text{Cu}$ milled 30 min is compared to the same composition cold rolled 5 times. Some characteristics presented by all other compositions are easily recognisable. First, the Bragg peaks of the ball milled sample are much broader than their counterparts of the cold rolled sample. This is an indication that the ball milled compound has smaller crystallites; an indication that 30 min of milling is more energetic than 5 cold rolls. We have to limit the number of rolling to 5 because in a previous investigation we have shown that higher number of rolling produce important oxidation and reduction of hydrogen capacity [26]. Second, the Bragg peaks of metastable phase $\gamma\text{-MgH}_2$ are present in the ball milled sample but barely visible in the cold rolled one. Again, this is an indication that ball milling 30 min is more energetic than 5 times rolling.

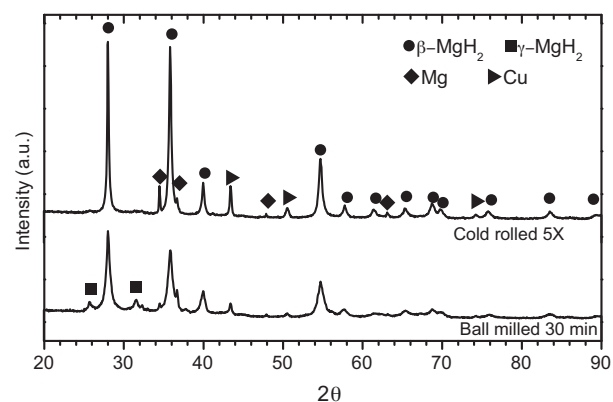


Fig. 1. X-ray powder diffraction of $\text{MgH}_2 + 2 \text{ at.}\% \text{Cu}$ processed by ball milling for 30 min and cold rolled 5 times.

Thirdly, a close inspection of the relative intensities of the $\beta\text{-MgH}_2$ peaks are not the same in ball milled and cold rolled samples. In the case of ball milled sample the relative intensities follows the reference pattern of $\beta\text{-MgH}_2$ but for the cold rolled sample there is some preferred orientation along the (0 1 1) direction. In fact, in order to have a meaningful Rietveld refinement preferred orientation along (0 1 1) should be refined. The same situation is seen for the Mg phase. In this case the preferred orientation is along (0 0 2).

Table 2

Crystallite size and microstrain of the $\beta\text{-MgH}_2$ phase and phase abundances in wt% as evaluated from Rietveld refinement of compounds ball milled 30 min in argon. For crystallite size and microstrain values in parenthesis are uncertainties on the last significant digit. For phase abundances error on all values is ± 1 . For some samples total do not add to 100 because of round-off.

| Catalyst | Abundance (wt%) | | | | Catalyst | $\beta\text{-MgH}_2$ | | Catalyst |
|----------|----------------------|-----------------------|----|-----|----------|----------------------|-----------------|----------|
| | $\beta\text{-MgH}_2$ | $\gamma\text{-MgH}_2$ | Mg | MgO | | Size (nm) | Microstrain (%) | |
| – | 80 | 8 | 4 | 9 | – | 19.5(5) | 0.78(4) | – |
| Co | 79 | 10 | 4 | 7 | Trace | 16.7(5) | 0.87(5) | – |
| Cr | 74 | 8 | 4 | 12 | 2 | 19.0(5) | 0.82(4) | 47(5) |
| Cu | 75 | 10 | 4 | 10 | 1 | 16.4(4) | 0.82(5) | 55(10) |
| Fe | 78 | 10 | 3 | 8 | 1 | 16.7(4) | 0.86(5) | 73(15) |
| Mn | 78 | 9 | 3 | 8 | 2 | 16.3(4) | 0.85(5) | 11(3) |
| NbH | 77 | 9 | 3 | 6 | 5 | 17.4(5) | 0.77(5) | 28(2) |
| Ni | 76 | 9 | 5 | 6 | 5 | 16.9(6) | 0.90(6) | 52(4) |
| Ti | 80 | 7 | 4 | 8 | Trace | 21.8(5) | 0.60(4) | – |
| V | 75 | 6 | 4 | 15 | Trace | 23.1(5) | 0.65(4) | – |

Table 3

Crystallite size and microstrain of the $\beta\text{-MgH}_2$ phase and phase abundances in wt% as evaluated from Rietveld refinement of compounds cold rolled 5 times in air. For crystallite size and microstrain values in parenthesis are uncertainties on the last significant digit. For phase abundances error on all values is ± 1 . For some samples total do not add to 100 because of round-off.

| Catalyst | Abundance (wt%) | | | Catalyst | $\beta\text{-MgH}_2$ | | Catalyst |
|----------|----------------------|----|-----------------------------|----------|----------------------|-----------------|----------|
| | $\beta\text{-MgH}_2$ | Mg | | | Size (nm) | Microstrain (%) | |
| – | 91 | 4 | 6 ($\gamma\text{-MgH}_2$) | 27.8(8) | 0.77(3) | – | |
| Co | 96 | 4 | Trace | 42(1) | 0.52(2) | – | |
| Cr | 95 | 4 | 2 | 29.4(8) | 0.72(3) | 21(2) | |
| Cu | 93 | 4 | 4 | 37(1) | 0.48(3) | 53(4) | |
| Fe | 94 | 4 | 3 | 35(1) | 0.58(3) | 42(4) | |
| Mn | 95 | 4 | 1 | 48(1) | 0.40(2) | 27(6) | |
| Nb | 94 | 4 | 3 | 42(1) | 0.42(2) | 27(2) | |
| Ni | 93 | 4 | 3 | 32(1) | 0.66(3) | 49(5) | |
| Ti | 96 | 4 | Trace | 46(1) | 0.49(2) | – | |
| V | 95 | 4 | 1 | 37(1) | 0.62(3) | 25(5) | |

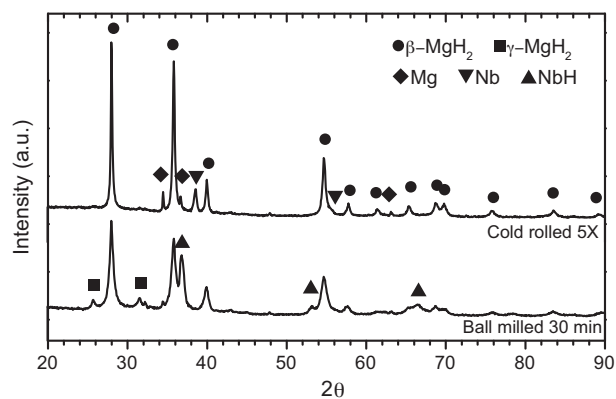


Fig. 2. X-ray powder diffraction of $\text{MgH}_2 + 2 \text{ at.}\% \text{Nb}$ processed by ball milling for 30 min and cold rolled 5 times.

as it is clear from Fig. 1, cold rolled spectra where the Mg peak at around 34° is much more intense than the (0 1 1) peak at around 36° . These preferred orientations are attributed to the effect of cold rolling and have been reported before [30]. The Bragg peaks from Cu are more visible in the pattern of the cold rolled sample than

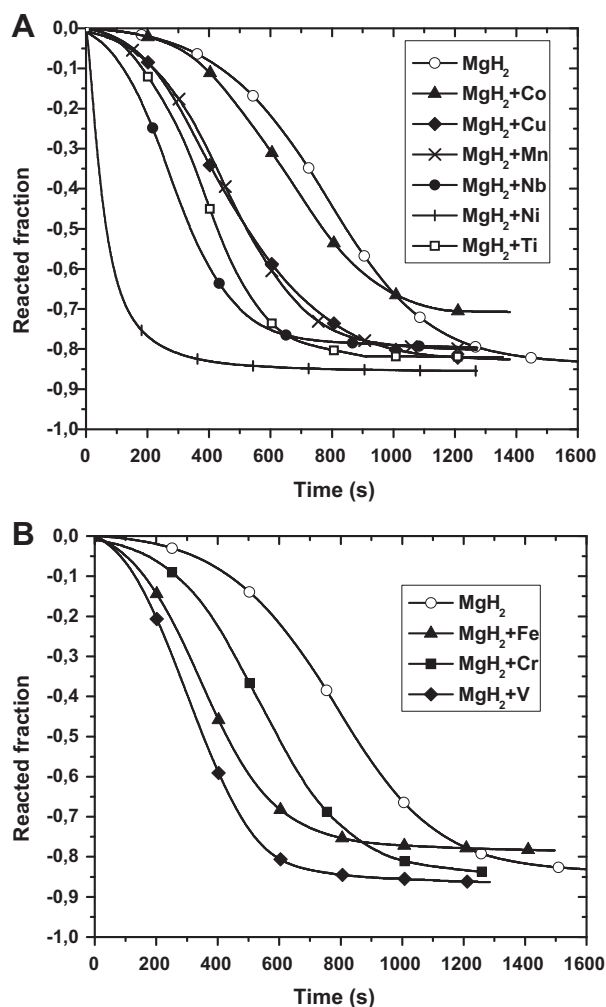


Fig. 3. Hydrogen desorption kinetics at 623 K under 35 kPa of hydrogen of $\text{MgH}_2 + 2 \text{ at.}\% \text{X}$ ball milled 30 min under argon. Capacities are expressed as fraction of theoretical maximum capacity (7.6 wt%). Weight of the catalyst was subtracted for the calculation of capacities. Data points were taken at every second. Symbols are shown only for curve identification. A: X = Co, Cu, Mn, Nb, Ni, and Ti; B: X = Cr, Fe, and V.

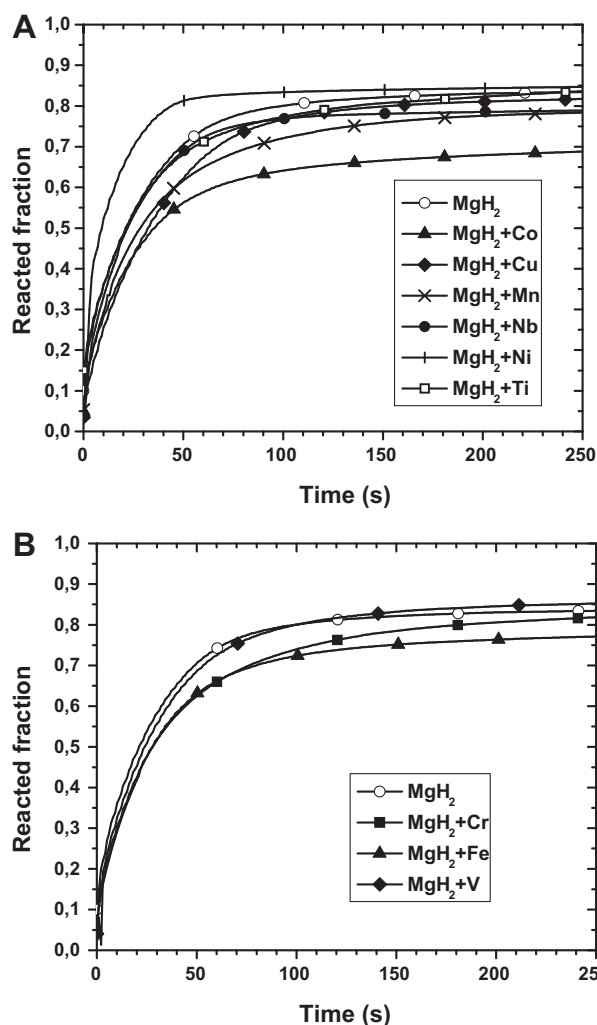


Fig. 4. Hydrogen absorption kinetics at 623 K under 2000 kPa of hydrogen of $\text{MgH}_2 + 2 \text{ at.}\% \text{X}$ ball milled 30 min under argon. Capacities are expressed as fraction of theoretical maximum capacity (7.6 wt%). Weight of the catalyst was subtracted for the calculation of capacities. Data points were taken at every second. Symbols are shown only for curve identification. A: X = Co, Cu, Mn, Nb, Ni, and Ti; B: X = Cr, Fe, and V.

the one ball milled. A similar situation was also seen for Fe catalyst. The reason is probably that ball milling 30 min is more energetic than cold rolling 5 times thus distributing the catalyst more finely in the MgH_2 and also a greater reduction of the catalyst's crystallite size. For Mn and Ni catalysts it is the ball milled sample that has stronger Bragg peaks attributed to the catalyst. Here the reason is that the particle sizes of these two catalysts are very small compare to MgH_2 particle size. This makes the mixing harder to achieve. Also during cold rolling the catalyst particles have a tendency of falling first through the rolling mill and do not bind well with MgH_2 . For the other catalysts the intensity is either the same or too small to be identified. A notable exception is with Nb catalyst which diffraction patterns are presented in Fig. 2. This figure shows the usual discrepancies between ball milled and cold rolled material, i.e. broader peaks for ball milled sample, presence of metastable $\gamma\text{-MgH}_2$ phase only in the ball milled sample, presence of texture in the cold rolled sample. However, in the cold rolled sample the Bragg peaks of Nb are clearly identified while for the ball milled sample they are totally absent and instead it is the NbH Bragg peaks that are present. This means that ball milling for 30 min is energetic enough to have the Nb 'pump out' hydrogen from MgH_2 to form the more stable hydride NbH. This is another proof that ball milling

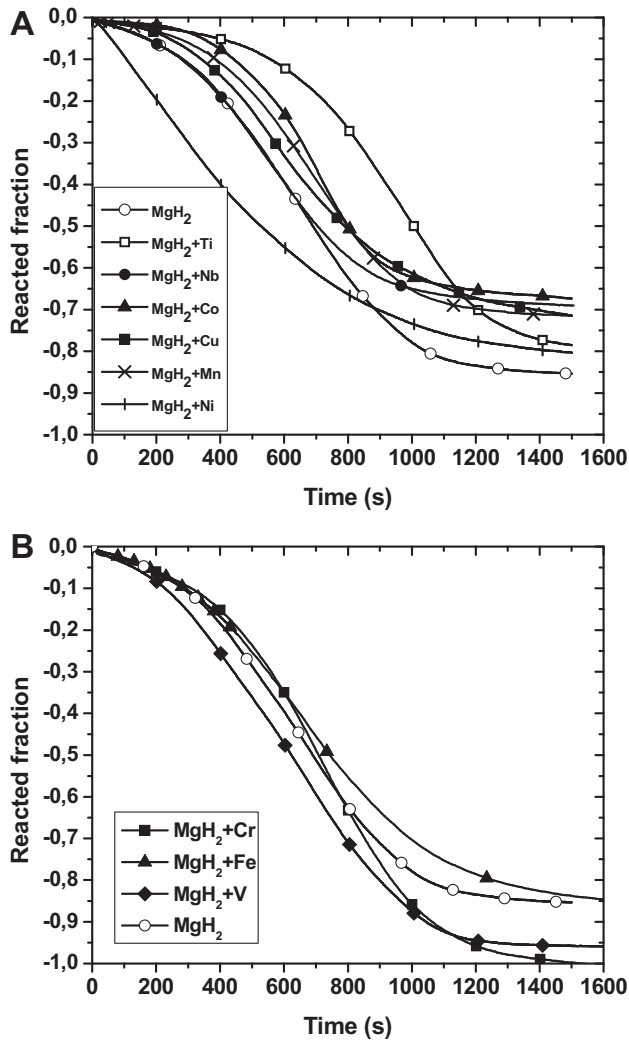


Fig. 5. Hydrogen desorption kinetics at 623 K under 35 kPa of hydrogen of $\text{MgH}_2 + 2 \text{ at.}\% \text{X}$ cold rolled 5 times in air. Capacities are expressed as fraction of theoretical maximum capacity (7.6 wt%). Weight of the catalyst was subtracted for the calculation of capacities. Data points were taken at every second. Symbols are shown only for curve identification. A: X = Co, Cu, Mn, Nb, Ni, and Ti; B: X = Cr, Fe, and V.

for 30 min is more energetic than cold rolling 5 times in the present conditions. The phase abundances, crystallite size and strain of $\beta\text{-MgH}_2$ as well as the crystallite size of catalysts as determined by Rietveld refinement and for samples prepared by ball milling and cold rolling are respectively shown in Tables 2 and 3. In the case of ball milled samples, the abundance of MgO varies between 7 and 12 wt%. For the cold rolled sample Bragg peaks of MgO were not identified. As explained in an earlier publication, the identification of MgO phase in the ball milled samples and not in the cold rolled ones may be due to the very small crystallite size in the later (of the order of a few nanometers) which makes the Bragg peaks extremely broad and essentially get them undistinguishable from the background [30]. Inspection of both tables shows that for each technique the phase's abundances as well as crystallite size and microstrain of $\beta\text{-MgH}_2$ are essentially the same for all compounds. In the case of ball milling the average crystallite size is 18.4 nm and microstrain 0.79% while for cold rolling they are respectively 37.6 nm and 0.57%. Thus, we have here another indication that ball milling 30 min is more energetic than rolling 5 times by the fact that the crystallite size is a factor two smaller and the microstrain more important in the ball milled compounds compared to the cold rolled ones. Finally, it should be pointed out that in the case of

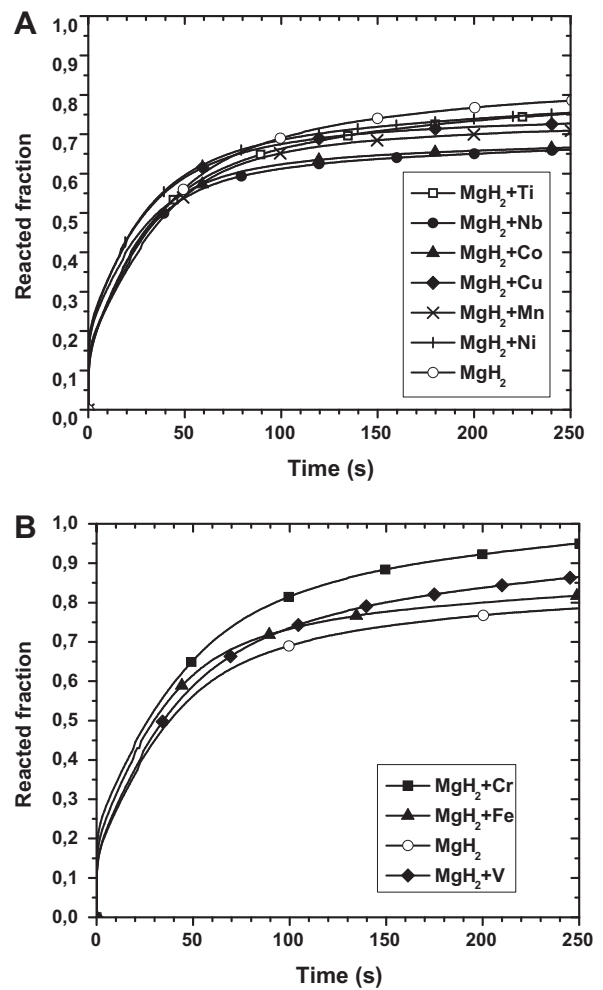


Fig. 6. Hydrogen absorption kinetics at 623 K under 2000 kPa of hydrogen of $\text{MgH}_2 + 2 \text{ at.}\% \text{X}$ cold rolled 5 times in air. Capacities are expressed as fraction of theoretical maximum capacity (7.6 wt%). Weight of the catalyst was subtracted for the calculation of capacities. Data points were taken at every second. Symbols are shown only for curve identification. A: X = Co, Cu, Mn, Nb, Ni, and Ti; B: X = Cr, Fe, and V.

cold rolling, it seems that addition of a catalyst reduces the rolling effectiveness. From Table 3 we see that rolling without catalyst resulted in a smaller crystallite size and higher microstrain with the formation of the metastable $\gamma\text{-MgH}_2$ phase. In previous investigations we also saw that cold rolling even for as small number of times as 5 resulted in the formation of the metastable $\gamma\text{-MgH}_2$ phase [26,30].

Despite the fact that rolling with a catalyst reduces the effectiveness of crystallite size reduction in $\beta\text{-MgH}_2$ phase it is still relatively effective in decreasing the crystallite size of the catalyst itself. As could be seen by comparing Tables 2 and 3, the catalyst crystallite size is the same as in ball milled compound for Cu, Nb, and Ni additions while it is smaller for Cr and Fe and bigger for Mn. However, care should be taken in interpretation of these results because the crystallite sizes were evaluated for minor phases. Nevertheless, the main fact is that cold rolling could also produce nanocrystalline structures in the catalytic species.

3.2. Hydrogen sorption properties

As the goal of this paper is to investigate the discrepancies between ball milling and cold rolling as a mean to add catalyst to MgH_2 we will first show the results pertaining to catalytic

addition by ball milling. These will serve as a reference for the samples processed by cold rolling.

3.2.1. Ball milled compounds

The dehydrogenation kinetics at 623 K for mixtures of $\text{MgH}_2 + 2 \text{ at.}\%X$ ($X = \text{Co, Cr, Cu, Fe, Mn, Nb, Ni, Ti, V}$) ball milled 30 min are shown in Fig. 3. For clarity of the presentation, two separated figures are used to report all results. The amount desorbed is expressed as a ratio of measured capacity over maximum theoretical capacity for each compound. Weight of catalyst was taken into account in evaluation of theoretical capacity. It is clear

that, under these milling conditions, all elements have some sort of catalytic activity but the effect varies greatly from one element to another. Catalytic activity of cobalt is minimal while nickel greatly reduces desorption time. In fact, close inspection shows that all curves have a sigmoid shape except for nickel. Apart from nickel, good catalysts are niobium, vanadium, and titanium.

Hydrogenation kinetics at 623 K under 2000 kPa of hydrogen is shown in Fig. 4. As for dehydrogenation, nickel is the best catalyst while cobalt is the worst. All other catalysts have minimal effect on the hydrogenation kinetic compared to uncatalyzed MgH_2 . We attribute this behaviour to the fact that the driving force (applied

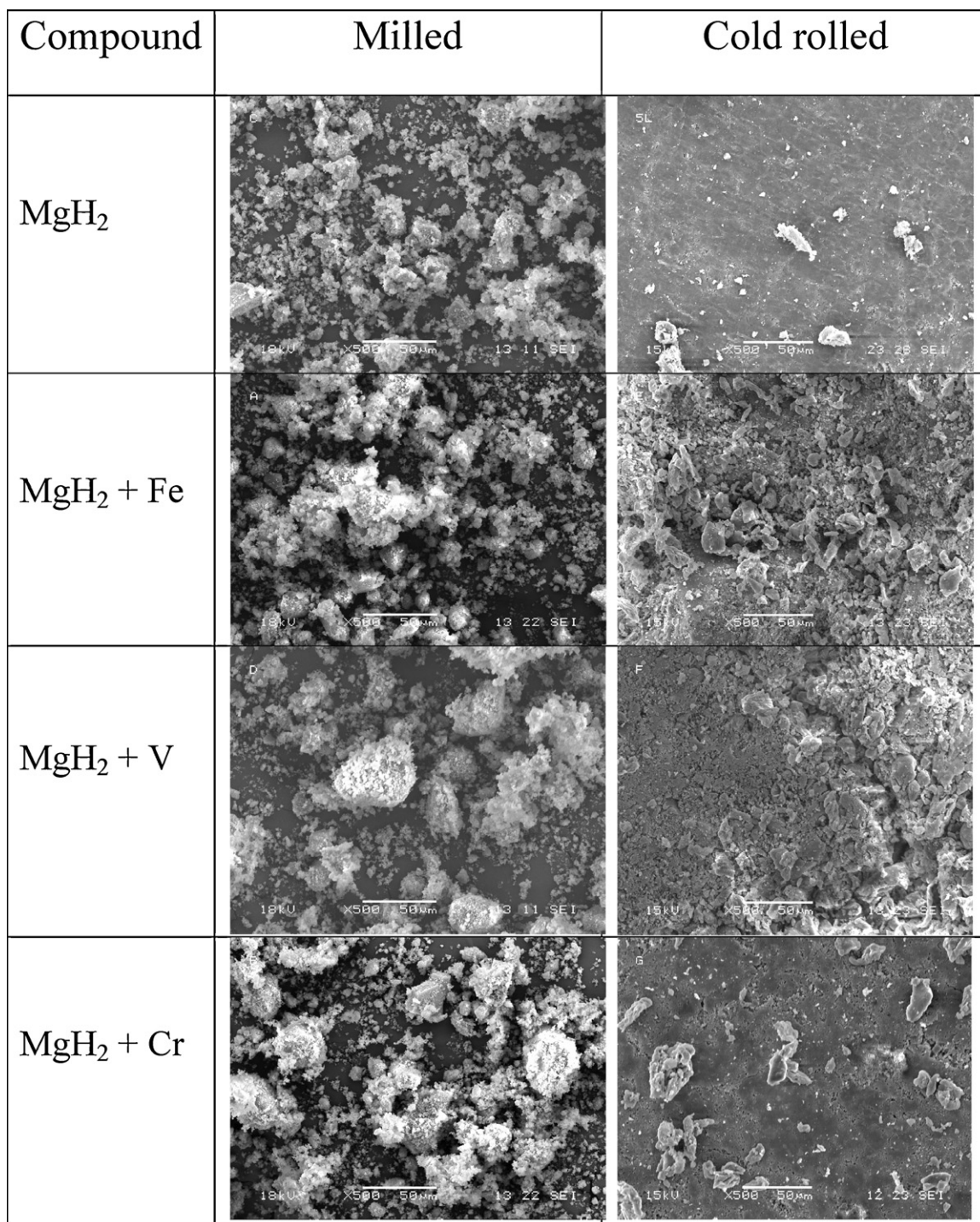


Fig. 7. Scanning electron microscope (SEM) micrographs of MgH_2 undoped and doped with Fe, Cr, and V. Left column: samples ball milled 30 min; right column: samples cold rolled 5 times. All micrographs are at magnification $\times 500$.

pressure compared to plateau pressure) was too high and actually was the dominant factor in hydrogenation. As the goal of this investigation is to compare ball milling with cold rolling in air, it could be interesting to see if cold rolled and ball milled samples have the same behaviour under high driving force.

3.2.2. Cold rolled compounds

The dehydrogenation kinetics of cold rolled samples are shown in Fig. 5. By comparing the kinetics of uncatalyzed MgH_2 in Figs. 5A and 3A we see that the cold rolled sample has a slightly faster desorption kinetics than the ball milled one. The reason for this behaviour is still unclear. Cold rolling certainly produces some particle size reduction but at the same time these particles are consolidated in small plates (see Section 3.3). Thus, the better kinetic may be a combination of smaller particle size and better heat transfer due to the consolidation of these particles in a small plate.

In general, the dehydrogenation kinetics of catalyzed MgH_2 are similar or even slower than uncatalyzed MgH_2 . As in the case of ball milling, all curves have a sigmoid shape except for nickel. Only vanadium and chromium catalyzed samples show faster kinetic and more complete desorption than uncatalyzed MgH_2 . For hydrogenation reaction, as shown in Fig. 6 all elements present a slower kinetic compare to pure MgH_2 with the exception of chromium, iron, and vanadium. What is surprising is to see that even nickel do not significantly improve absorption kinetic. But, as pointed out for the ball milled samples, the high driving force may make the comparison difficult. Despite this limitation, it is clear that addition of catalyst by cold rolling only 5 times is not as efficient as ball milling 30 min.

The reason why addition of catalysts by cold rolling did not improved sorption kinetics is most probably due to the inefficiency of getting a close contact of the catalyst with MgH_2 . As pointed out before, for some catalysts the difference between particle size of the catalyst and MgH_2 is quite important and leads to a segregation during rolling. Also, only 5 rolls are most probably not sufficient to obtain a good binding between the catalyst and MgH_2 . Most probably a higher number of rolls would lead to a positive effect of catalysts on hydrogen sorption properties of MgH_2 but this could not be performed in air due to excessive oxidation of the hydride as shown in Ref. [26].

3.3. Scanning electron microscopy

Fig. 7 presents the micrographs of samples showing the best hydrogen sorption kinetics, i.e. MgH_2 doped with Fe, Cr, and V. In the case of ball milled samples doped with Fe, Cr, and V the particle size distribution is roughly the same. A totally different situation is seen for the cold rolled samples. After rolling, the magnesium hydride gets consolidated in small plates but the SEM micrographs clearly show that the porosities of these plates are different. We see that cold rolling the undoped MgH_2 resulted in a plate well consolidated while the doped MgH_2 have some porosities in the plates. A possible explanation could be that when a doping material is added, cold rolling is not as effective to consolidate the particles in plates.

4. Conclusion

We compared ball milling and cold rolling techniques as a mean to add transition metal catalysts to magnesium hydride. High energy ball milling was performed under argon for 30 min while cold rolling was done in air with a number of roll limited to five. Despite these discrepancies in the processing atmosphere the resulting kinetics were quite similar between cold rolled and ball milled samples. The ball milled samples showed smaller crystallite sizes (broader Bragg peaks in the X-ray diffraction patterns)

and smaller particle sizes which made the hydrogenation kinetics faster than their cold rolled samples but not by a wide margin. More specifically, the same transition elements (Ni, V, Nb) gave the fastest dehydrogenation kinetics for both methods. This work shows that cold rolling could be used to add catalysts to magnesium hydride. However, to have optimum effect the rolling should most probably be done under inert atmosphere. In this way, oxidation will be eliminated and more rolling passes could be performed thus reducing the crystallite and particles sizes to values comparable to the ones obtained by ball milling and getting a better distribution of the catalyst in the magnesium hydride matrix. It could be then expected to have hydrogen sorption properties similar to the ones obtained by ball milling.

Acknowledgements

This work was funded by the Natural Sciences and Engineering Research Council of Canada (NSERC). S. Vincent would like to thank Hydro-Québec for a summer fellowship.

References

- [1] J. Huot, G. Liang, S. Boily, A.V. Neste, R. Schulz, *Journal of Alloys and Compounds* 293–295 (1999) 495–500.
- [2] G. Liang, J. Huot, S. Boily, A.V. Neste, R. Schulz, *Journal of Alloys and Compounds* 292 (1999) 247–252.
- [3] M. Dornheim, S. Doppiu, G. Barkhordarian, U. Boesenberg, T. Klassen, O. Gutfleisch, R. Bormann, *Scripta Materialia* 56 (2007) 841–846.
- [4] A. Vaichere, D.R. Leiva, T.T. Ishikawa, W.J. Botta, *Materials Science Forum* 570 (2008) 39–44.
- [5] W. Oelerich, T. Klassen, R. Bormann, *Journal of Alloys and Compounds* 315 (2001) 237–242.
- [6] J.F.R.d. Castro, A.R. Yavari, A. LeMoulec, T.T. Ishikawa, W.J. Botta, *Journal of Alloys and Compounds* 389 (2005) 270–274.
- [7] N. Hanada, T. Ichikawa, H. Fujii, *Journal of Alloys and Compounds* 446–447 (2007) 67–71.
- [8] M. Dornheim, N. Eigen, G. Barkhordarian, T. Klassen, R. Bormann, *Advanced Engineering Materials* 8 (2006) 377–385.
- [9] V. Skripnyuk, E. Buchman, E. Rabkin, Y. Estrin, M. Popov, S. Jorgensen, *Journal of Alloys and Compounds* 436 (2007) 99–106.
- [10] V. Skripnyuk, E. Rabkin, Y. Estrin, R. Lapovok, *Acta Materialia* 52 (2004) 405–414.
- [11] V.M. Skripnyuk, E. Rabkin, Y. Estrin, R. Lapovok, *International Journal of Hydrogen Energy* 34 (2009) 6320–6324.
- [12] Y. Kusadome, K. Ikeda, Y. Nakamori, S. Orimo, Z. Horita, *Scripta Materialia* 57 (2007) 751–753.
- [13] G.F. Lima, A.M. Jorge, D.R. Leiva, C.S. Kiminami, C. Bolfarini, W.J. Botta, in: L. Schultz, J. Eckert, L. Battezzati, M. Stoica (Eds.), *13th International Conference on Rapidly Quenched and Metastable Materials*, Iop Publishing Ltd., Bristol, 2009, p. 12015.
- [14] T.T. Ueda, M. Tsukahara, Y. Kamiya, S. Kikuchi, *Journal of Alloys and Compounds* 386 (2004) 253–257.
- [15] K. Tanaka, N. Takeichi, H. Tanaka, N. Kuriyama, T.T. Ueda, M. Tsukahara, H. Miyamura, S. Kikuchi, *Journal of Materials Science* 43 (2008) 3812–3816.
- [16] N. Takeichi, K. Tanaka, H. Tanaka, T.T. Ueda, Y. Kamiya, M. Tsukahara, H. Miyamura, S. Kikuchi, *Journal of Alloys and Compounds* 446–447 (2007) 543–548.
- [17] K. Saganuma, H. Miyamura, S. Kikuchi, N. Takeichi, K. Tanaka, H. Tanaka, N. Kuriyama, T.T. Ueda, M. Tsukahara, *Advanced Materials Research* 26–28 (2007) 857–860.
- [18] R. Mori, H. Miyamura, S. Kikuchi, K. Tanaka, N. Takeichi, H. Tanaka, N. Kuriyama, T.T. Ueda, M. Tsukahara, *Materials Science Forum* 561–565 (2007) 1609–1612.
- [19] J. Dufour, J. Huot, *Journal of Alloys and Compounds* 439 (2007) L5–L7.
- [20] J. Dufour, J. Huot, *Journal of Alloys and Compounds* 446–447 (2007) 147–151.
- [21] L.T. Zhang, K. Ito, V.K. Vasudevan, M. Yamaguchi, *Acta Materialia* 49 (2001) 751–758.
- [22] L.T. Zhang, K. Ito, V.K. Vasudevan, M. Yamaguchi, *Materials Science and Engineering A* 329–331 (2002) 362–366.
- [23] S. Amira, S.F. Santos, J. Huot, *Intermetallics* 18 (2010) 140–144.
- [24] S. Couillaud, H. Enoki, S. Amira, J.L. Bobet, E. Akiba, J. Huot, *Journal of Alloys and Compounds* 484 (2009) 154–158.
- [25] D.R. Leiva, A.M. Jorge, T.T. Ishikawa, J. Huot, D. Fruchart, S. Miraglia, C.S. Kiminami, W.J. Botta, *Advanced Engineering Materials* 112 (2010) 786–792.
- [26] J. Lang, J. Huot, *Journal of Alloys and Compounds* 509 (2011) L18–L22.
- [27] S.D. Vincent, J. Huot, *Journal of Alloys and Compounds* 509 (2011) L175–L179.
- [28] BRUKER-AXS, TOPAS V4: General Profile and Structure Analysis Software for Powder Diffraction Data, Bruker AXS, Karlsruhe, Germany, 2008.
- [29] R.W. Cheary, A.A. Coelho, J.P. Cline, *Journal of Research of the National Institute of Standard and Technology* 109 (2004) 1–25.
- [30] M. Tournant, J. Huot, *Solid State Phenomena* 170 (2011) 144–149.